JOURNAL OF AIRCRAFT
Vol. 41, No. 3, May–June 2004

Shock-Wave/Boundary-Layer Interaction Control Using Streamwise Slots in Transonic Flows

A. N. Smith* and H. Babinsky†
University of Cambridge, Cambridge, England CB2 1PZ, United Kingdom
J. L. Fulker‡
QinetiQ, Bedford, England MK 41 6AE, United Kingdom
and
P. R. Ashill§
Cranfield College of Aeronautics, Bedfordshire, England MK43 OAL, United Kingdom

The effect of streamwise slots on the interaction of a normal shock wave with a turbulent boundary layer has been investigated experimentally at a Mach number of 1.29. The surface-pressure distribution for the controlled interaction was found to feature a distinct plateau. This was caused by a change in shock structure from a typical unseparated normal shock-wave/boundary-layer interaction to a large bifurcated lambda-type shock pattern, which led to a reduction of total pressure losses. A strong spanwise variation of boundary-layer properties was observed downstream of the slots, whereas the modified shock structure was relatively two-dimensional. Surface flow visualization confirmed that the slots introduced a region of recirculation into the boundary layer, similar to passive control with uniform surface ventilation. Surface flow visualization revealed the presence of a pair of counter-rotating vortices, confirmed by crossflow velocity measurements. Because of the reduction of total pressure losses, streamwise slots can reduce aircraft wave drag at transonic cruise while incurring only small viscous penalties. A similar control device can also be of use in supersonic intakes where total pressure losses limit engine performance. The introduction of streamwise vorticity can be beneficial in delaying boundary-layer separations often encountered in intakes and on transonic wings. The device is also thought to be capable of delaying buffet onset.

Nomenclature

M	=	Mach number
P	=	pressure
U	=	streamwise velocity
x	=	streamwise distance, mm
y	=	vertical distance, mm
z	=	spanwise distance, mm
δ	=	boundary-layer thickness

Subscripts

S	=	surface static value
0	=	total value
1	=	upstream value
2	=	downstream value

Introduction

NORMAL shock-wave/boundary-layer interactions occur on civil transport and military aircraft wings at cruise Mach numbers and during high-performance maneuvers. The flow over the upper surface of the wing usually exhibits a large region of supersonic flow, which is terminated by a normal shock wave. Typical shock Mach numbers are in the range 1.1–1.4, causing wave drag, and in the case of stronger shocks boundary-layer separation (and hence loss of lift). Strong interactions can also lead to buffeting. In practice these effects are minimized by limiting the maximum flow speed on the aircraft wing through design of the airfoil section and restricting the maximum flight Mach number of the aircraft. Recent research efforts into shock-wave/boundary-layer interaction control have focused on methods to smear the shock-induced pressure rise and thereby reduce its damaging effect on the boundary layer. More importantly, smearing of the shock wave, or replacing a rapid pressure rise with a series of smaller jumps, is also responsible for a reduction in wave drag. Examples of control are passive devices[1–3] using a perforated plate, active control,[4–6] blowing,[7] or more commonly suction,[7,8] or geometrical modifications, that is, bumps.[9–11] The primary aim of all of these devices is to reduce wave drag. Passive control has been shown to incur large viscous penalties (although it has potential to delay buffet onset[12–14]), whereas the benefits of applying suction and blowing have yet to be proven. Bumps would appear the most promising, incurring only a small viscous penalty at worst. However they are only effective at the design condition and in general would probably need some form of variable geometry. This paper investigates the potential of a novel control mechanism, namely, streamwise slots.

Experiments performed on a two-dimensional transonic aerofoil by Ashill and Fulker[10] revealed that an aerofoil fitted with a control device consisting of streamwise slots demonstrated an increase in lift and a decrease in drag at high angles of attack. In addition, a delay in the divergence of trailing-edge pressures was observed, indicating that the control device might help to delay trailing-edge separation, possibly through the introduction of streamwise vortices, similar to vortex generators.[15,16] Such a delay in trailing-edge pressure divergence is also likely to postpone buffet onset.[12]

However these results do not explain the physical mechanisms of the slot control device. Further research is needed to understand the shock-wave/boundary-layer interaction flowfield in the presence of streamwise slots. This paper describes experiments of a more fundamental nature to aid this understanding.

Received 25 August 2001; revision received 4 November 2002; accepted for publication 4 November 2002.

*Research Student, Department of Engineering, Trumpington Street.
†Senior Lecturer in Aerodynamics, Department of Engineering, Trumpington Street. Member AIAA.
‡Technology Chief, Aircraft Aerodynamics, Centre for Aerospace Technology. Member AIAA.
§Visiting Professor, Cranfield College of Aeronautics. Member AIAA.

Experimental Arrangement

The experimental investigation was undertaken in the supersonic wind tunnels of the Department of Engineering at Cambridge University. The tunnel arrangement and control device are shown in Fig. 1. The control device (shown in the inset) was fitted above a cavity of depth 38 mm in the floor of the rectangular working section (0.114×0.179 m). The slot width was scaled (using the boundary-layer displacement thickness) to be equivalent to the configuration reported in Ref. 10. The spanwise spacing between slots was 44 mm. To visualize the vertical flow in and out of the slots, a splitter plate (10 mm high, 0.5 mm wide) was fitted in the center of the middle slot in some experiments.

By manually adjusting the freestream stagnation pressure, a recovery shock wave was held at a given location above the slotted surface. The tunnel was operated at a Mach number of 1.29 and a freestream unit Reynolds number of 32×10^6/m. Surface oil flow visualization was performed using a mixture of paraffin, titanium dioxide, and oleic acid. Surface-pressure measurements were made by connecting pressure tappings to Druck PDCR-200 miniature pressure transducers, the locations of which are shown in Fig. 2 by the cross symbols, together with the coordinate system used for all measurements. The streamwise coordinate x is measured from the center of the wind-tunnel window, the vertical distance y is measured from the wind-tunnel floor, and the spanwise coordinate z is measured from the wind-tunnel centerline.

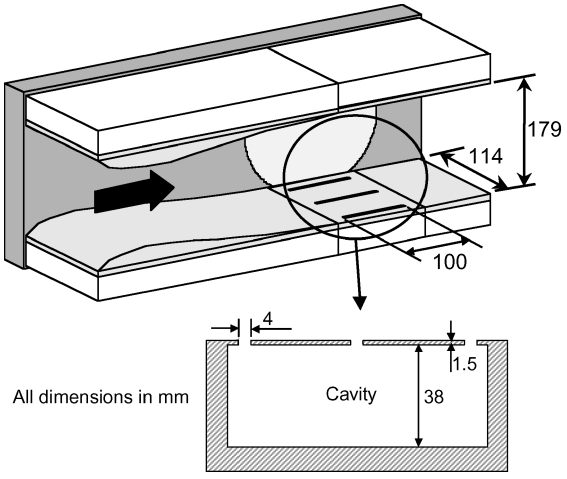

Fig. 1 Wind-tunnel arrangement.

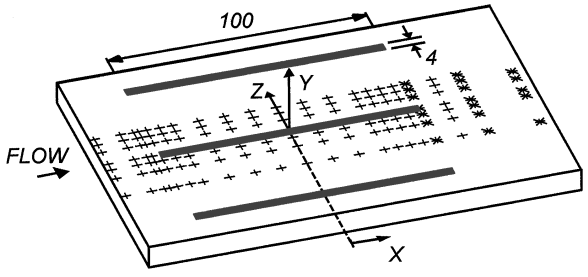

Fig. 2 Coordinate system and measurement positions (+, surface pressure; ∗, boundary-layer traverse).

Boundary-layer traverses were performed using a flat-head pitot probe (dimensions of 1.61×0.131 mm) and a three-hole probe (dimensions of 1.91×0.64 mm, outer tubes angled at 45 deg), connected to pressure transducers. Traverses were performed at three streamwise stations ($x = 50$, 70, and 90 mm) downstream of the interaction, and at varying spanwise locations, shown by the star symbols in Fig. 2. A pitot-pressure probe was also used with a round head of diameter 1.1 mm.

Experimental Accuracy

Surface static and pitot pressures were measured with fast-response pressure transducers, and the experimental error of these measurements is of the order of $\pm 1\%$. The accuracy of the traverse gear used in the determination of boundary-layer profiles was better than 0.1 mm (0.5% of δ). The accuracy of the traverse gear used for the pitot-pressure traverses was better than 1.5 mm (1.5% of the maximum traverse height). However, when evaluating velocity profiles from pitot-pressure measurements in compressible flow a number of assumptions are commonly made, and particularly near the surface, probe interference effects are likely to introduce uncertainties into the final data. Although it is not generally possible to quantify these errors, it is thought that velocity information is likely to suffer from uncertainties of the order of $\pm 5\%$ in the outer regions and $\pm 10\%$ in the inner regions ($y < 1$ mm) of the boundary layers.

The three-hole probe was calibrated for flow angles ranging from -20 to 20 deg and for Mach numbers ranging from 0.3–0.8. The flow angle is likely to suffer from uncertainties of $\pm 5\%$ in the outer regions, whereas in the near-wall region the size of the probe leads to errors, and it is estimated that here the flow is likely to suffer uncertainties of the order of $\pm 15\%$.

The location of the shock wave itself is subject to uncertainties. A degree of unsteadiness was observed, resulting in an error in streamwise location of the order of ± 3 mm, which is typically 3% of the length of the control device.

During surface-pressure measurements, the results were found to be repeatable to 2% accuracy, whereas boundary-layer velocity measurements were repeatable to 5% accuracy.

Results

Uncontrolled Shock-Wave/Boundary-Layer Interaction

Figure 3 shows a schlieren picture of an uncontrolled shock-wave/boundary-layer interaction located in the center of the test section. The flowfield is typical for an unseparated interaction as described by Atkin and Squire,[17] with a small degree of smearing occurring at the shock foot. A spurious wave can be seen to emanate from upstream of the interaction; this is caused by small imperfections in the tunnel walls. Such waves are very weak and do not influence the flowfield significantly.

Shown alongside the schlieren picture is the total pressure profile, measured downstream of the interaction at $x = 90$. Three distinct regions in the profile can be identified. In the range $0 < y < 10$ a

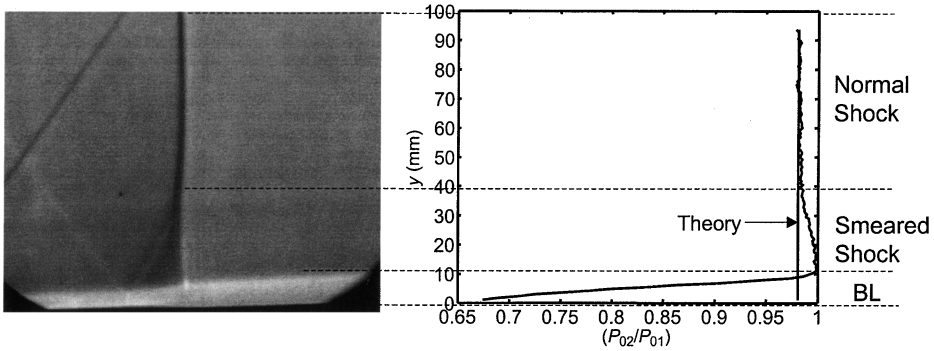

Fig. 3 Schlieren picture and total pressure profile for uncontrolled interaction.

large total pressure loss can be observed, which corresponds to the boundary-layer region. Above $y \approx 35$ the total pressure is consistent with the theoretical value ($P_{02}/P_{01} = 0.981$), behind a normal shock at $M = 1.29$, illustrated in Fig. 3. In between the total pressure loss is reduced to almost zero at $y \approx 20$. This is caused by the natural shock smearing close to the boundary-layer edge, where the shock is replaced by a series of compression waves.

Surface static pressures were measured at various spanwise locations, and the uncontrolled interaction was found to be relatively uniform across the working section, apart from the regions closest to the sidewalls.

The incoming boundary-layer profile was measured at $x = -53$. The boundary-layer edge was determined using the Childs wall/wake fit,[18] and the boundary-layer thickness was found to be 6.7 mm. The boundary-layer velocity data were compared to Coles law of the wall,[19] and a good agreement was obtained indicating that the incoming profile is typical of a flat-plate equilibrium turbulent boundary layer. Boundary-layer velocity profiles measured at various spanwise positions downstream of the interaction confirmed that the datum interaction is nominally two-dimensional. The average boundary-layer thickness downstream of the interaction ($x = 70$) was found to be 10.8 mm.

Slot-Controlled Interaction

Figure 4 shows a schlieren photograph, where the shock was located above the center of the slots at $x = 0$. It can be seen that a lambda-type shock structure is formed with the leading leg originating from the upstream edge of the slot. It is thought that blowing from the upstream region of the slots is responsible for the change in shock structure. Further downstream two distinct boundary-layer edges can be observed in the schlieren picture, indicating that the boundary-layer thickness is not uniform in the spanwise direction.

Surface-pressure measurements (Fig. 5) show a distinct plateau in the pressure rise, typical for a lambda shock structure. Experimental investigations with passive control have shown that such a structure can reduce the total pressure loss through the shock wave[4,20] and lead to a wave drag reduction on transonic wings.[2]

The surface-pressure map for the controlled interaction is shown in Fig. 6. It can be seen that with increasing spanwise distance from the slot, the initial pressure rise occurs further downstream, indicating that the leading shock front is slightly three-dimensional. The location of the pressure rise from the rear leg occurs further upstream with increasing distance from the slot, suggesting that with increasing distance from the slot the interaction relaxes towards an uncontrolled interaction. However this relaxation is relatively slow, and the effect of the slots on the shock structure is likely to persist for considerable spanwise distances.

Figure 7 shows surface oil flow visualisation for the controlled interaction. Flow can be seen to leave the slots in the upstream 50% of the slot indicating blowing, and flow can be seen to enter the slot in the downstream 50% of the slot, indicating suction. A separation line can be seen to extend from the leading edge of each slot. The presence of crossflow moving away from the slot towards the separation line, suggests the presence of a pair of counter-rotating vortices. It is thought that these vortices originate from the leading-edge regions of the slots. The strength of the vortices is intensified by the combined effects of suction and blowing along the length of the slot.

The presence of suction and blowing and its effect on the inviscid flowfield is demonstrated clearly when superimposing the splitter plate oil flow with a schlieren picture (Fig. 8). Here it can be seen that

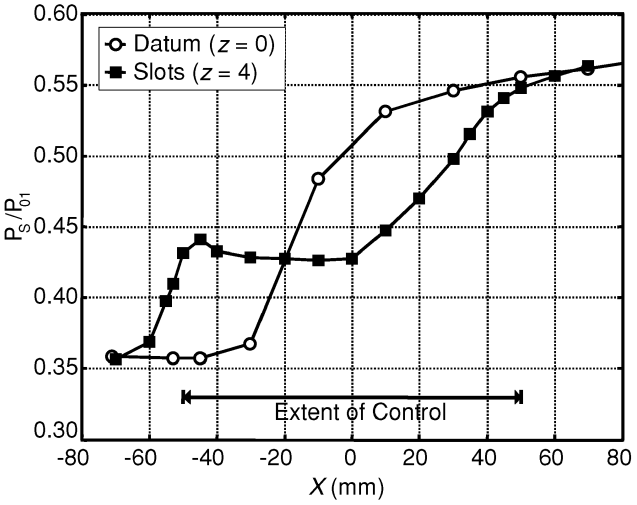

Fig. 5 Comparison of surface-pressure distributions for uncontrolled and controlled interaction.

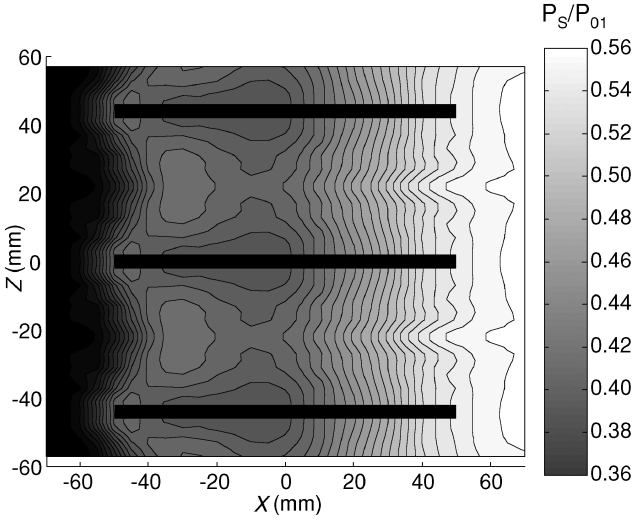

Fig. 6 Surface-pressure map (slot-controlled interaction).

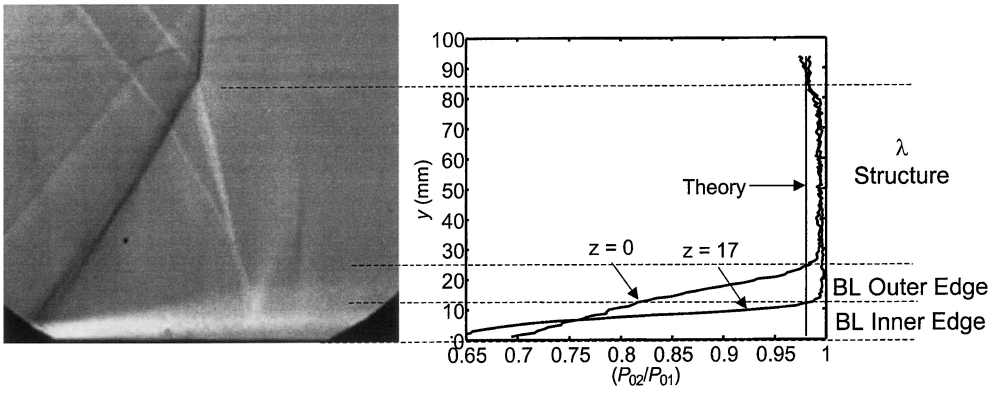

Fig. 4 Schlieren picture and total pressure profile for slot-controlled interaction.

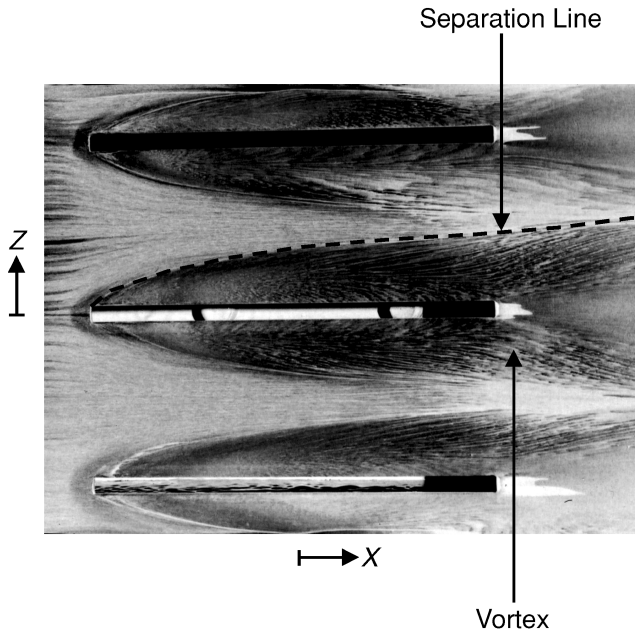

Fig. 7 Surface oil flow (slot-controlled interaction).

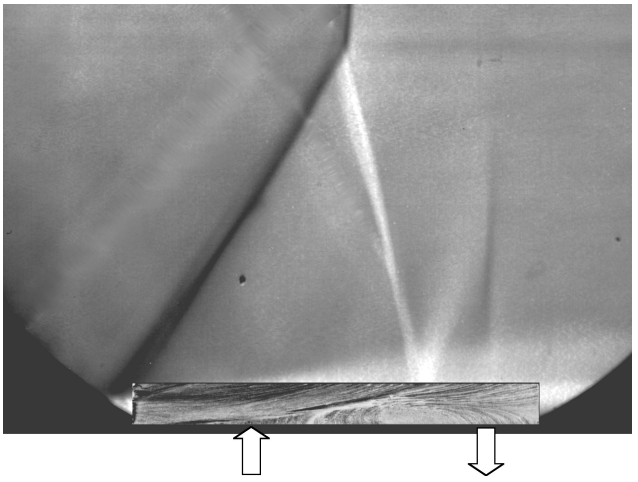

Fig. 8 Schlieren with splitter plate oil flow visualization for slot-controlled interaction.

the flow is deflected upwards in the upstream 50–70% of the slot, and there is clear evidence of flow into the slot in the downstream portion. The upstream deflection away from the wall of the oil flow is roughly parallel to the extreme edge of the boundary layer seen in the schlieren picture. The upstream onset of this deflection coincides with the leading leg of the lambda shock structure confirming that blowing from the slot is responsible for the change in the shock structure.

To measure the extent of crossflow and to confirm the presence of a streamwise vortex, a three-hole probe was used to survey the flow downstream of the slots. Figure 9 shows data measured at $x = 70$ and at varying spanwise locations.

Directly behind the slot ($z = 0$) and halfway between two slots ($z = 22$), there is little or no spanwise velocity component, confirming that the flow is symmetrical (consistent with the surface oil flow). In between, the flow close to the surface can be seen to be moving away from the slots, which is also consistent with the surface oil flow (Fig. 7). Further away from the surface, flow can be seen to move towards the slot, indicating the presence of a streamwise vortex, the center of which appears to be located at approximately $z = 6$.

Figure 10 shows boundary-layer velocity profiles measured at a streamwise location of $x = 50$ (the trailing edge of the slots) and

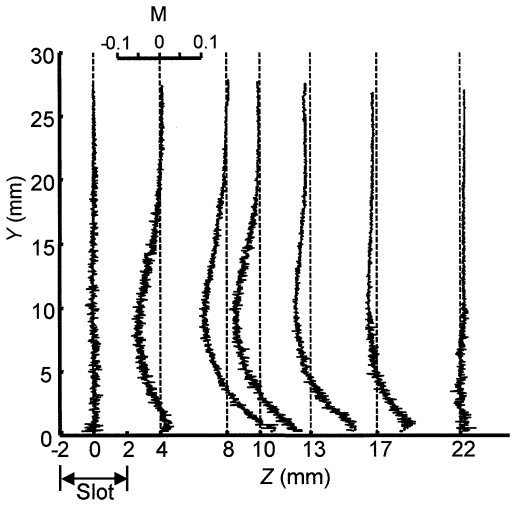

Fig. 9 Crossflow Mach-number profiles (slot-controlled interaction).

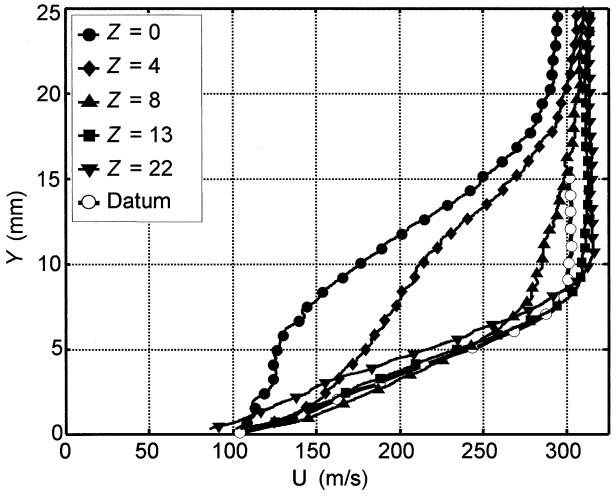

Fig. 10 Boundary-layer velocity profiles: $x = 50$ (slot-controlled interaction).

at various spanwise positions. It can be seen that there is a significant spanwise variation in boundary-layer thickness. Behind the slot ($z = 0$) the boundary-layer thickness is greatest, and the profile is considerably less full than at other spanwise locations. Further away from the slots the profile is fuller and thinner and comparable to that behind the datum interaction.

Boundary-layer velocity profiles measured further downstream at $x = 70$ (Fig. 11) reveal that the boundary-layer profile behind the slots is now fuller but still relatively thick, whereas further away from the slots the profile is still thin but becoming less full. Velocity profiles measured at $x = 90$ (Fig. 12) indicate that this trend continues. Such behavior is thought to be consistent with increased mixing as a result of the presence of streamwise vortices.[21,22]

Figure 13 is a graphical representation of the variation of boundary-layer thickness throughout and downstream of the interaction. (Values between $x = -50$ and 50 are interpolated.) Directly behind the slots the boundary layer is thickened considerably, whereas between the slots the boundary layer remains thin and is comparable to the datum interaction. Although the slots considerably thicken the boundary layer, this thickening is however confined to a narrow region. This boundary-layer thickness distribution is consistent with the "double edge" observed in the schlieren picture of Fig. 4.

Referring back to Fig. 4, two total pressure profiles measured at $x = 90$ are shown alongside the schlieren picture. These profiles were measured at two spanwise locations, directly behind the slots ($z = 0$) and almost halfway between slots ($z = 17$). Three distinct

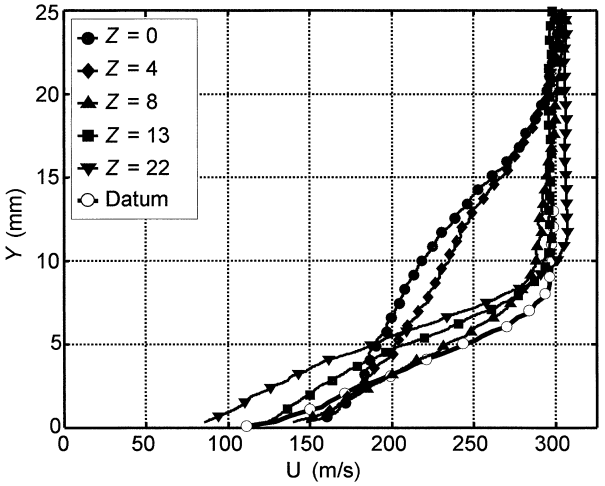

Fig. 11 Boundary-layer velocity profiles: $x = 70$ (slot-controlled interaction).

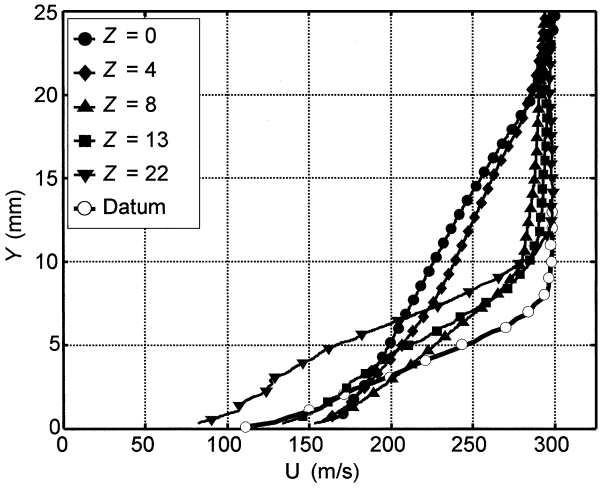

Fig. 12 Boundary-layer velocity profiles: $x = 90$ (slot-controlled interaction).

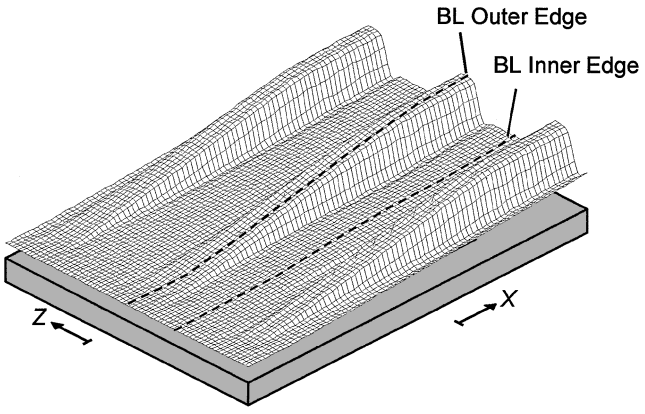

Fig. 13 Variation of boundary-layer thickness (slot-controlled interaction).

regions of pressure loss can be observed. In the inner region a total pressure loss caused by the presence of the boundary layer can be seen. This loss is greater for the thicker boundary-layer profile located behind the slot. The total pressure loss in the boundary layer for the profile located between slots is comparable to the datum interaction. The two boundary-layer edges that can be observed in the schlieren picture are seen to compare well with edge of the inner regions of total pressure loss.

Between the boundary-layer edge and the triple point a large reduction in total pressure loss compared to the normal shock value can be seen in the lambda shock region. This region extends to a similar height for both profiles confirming that the shock structure changes only slowly with spanwise distance. Above the triple point the total pressure loss is consistent with the theoretical normal shock value ($P_{02}/P_{01} = 0.981$) at a Mach number of 1.29, which is shown in Fig. 4.

Shown in Fig. 14 is the spanwise variation in total pressure loss, alongside the datum variation. It can be seen that the reduction in total pressure loss caused by the lambda shock structure extends well into the flow and is almost constant across the span. An increase in total pressure loss behind the slots caused by increased viscous losses is apparent, but with increasing spanwise distance away from the slots this pressure loss is reduced and is comparable to the datum interaction.

In summary, slots bifurcate the shock wave, thus potentially reducing wave drag on a transonic wing. The slots increase the viscous drag, but this increase is confined to a narrow region. The benefit of the bifurcated lambda shock structure is seen in the total pressure profiles, indicating that slots might have other applications other than aerofoil flow control, that is, in engine intakes. The streamwise slots also cause the formation of streamwise vortices, which increase mixing. Research into the use of vortex generators has shown similar boundary-layer behavior,[15,22] which when applied to a transonic aerofoil results in a delay of trailing-edge separation.[15,16] The main flowfield features of the interaction are illustrated in Fig. 15.

When applied to a wing, slots can be expected to reduce wave drag, slightly increase viscous drag, and delay trailing-edge separation, thereby leading to higher maximum lift coefficients. These results are consistent with the observations of Ref. 10.

Effect of Shock Location

For an aircraft in cruise, the shock wave on the wing will typically move and not remain in one fixed position,[23] and it is desirable that a control is effective over a range of shock locations.

Schlieren pictures of the shock located at $x = -17$ and 17 are shown in Fig. 16. The shock is bifurcated in both cases, and it can be seen that the strength of the leading leg appears to decrease as the shock wave moves downstream over the control device. The schlieren pictures suggest a three-dimensional boundary layer for all shock positions. Surface-pressure measurements (Fig. 17) confirm the decreasing strength of the leading leg with increasing streamwise location.

Boundary-layer velocity profiles for both shock locations, measured downstream of the interaction ($x = 90$), are shown in Fig. 18. It can be seen that the main characteristics are the same as those observed with shock wave located at $x = 0$, namely, that boundary-layer thickening is confined to a narrow spanwise region. The results indicate that shock location has a limited effect upon the boundary layer. Crossflow velocity measurements and surface flow visualization also indicated that the same flowfield features as in the datum control case are present.

When considering the effectiveness of the control to reduce total pressure losses, two factors must be considered: first, the height to which the lambda structure extends into the flow and second, the pressure ratio across each leg. When the shock is located in the forward position, the height of the lambda structure is reduced, and as a result the overall reduction in total pressure loss is not as great. When the shock wave is located in the rear position, the lambda structure extends well into the flow, providing a benefit over a greater height, but the front leg of the structure is relatively weak. This is likely to result in a smaller reduction in total pressure loss.

Other control devices (suction and bumps) are often only effective at one design condition, whereas the slot control device appears to be effective at a range of shock locations. However there is likely to be an optimum shock location as a result of the tradeoff between the strength of the leading leg and the height of the lambda structure.

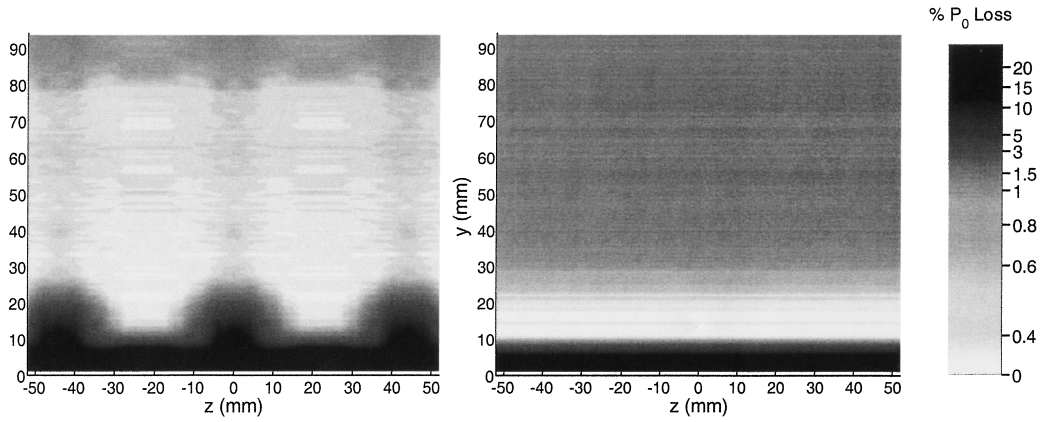

a) b)

Fig. 14 Spanwise variation of total pressure: a) controlled and b) uncontrolled.

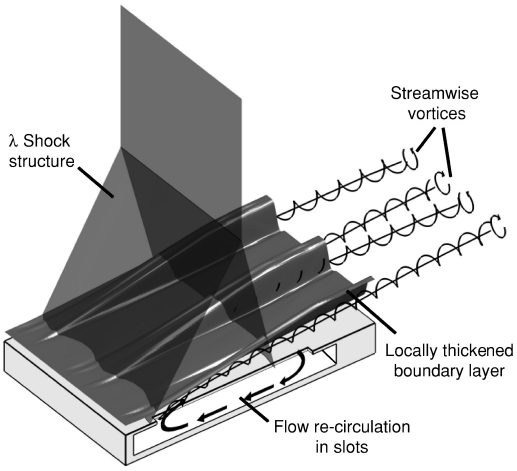

Fig. 15 Key features of slot-controlled interaction flowfield.

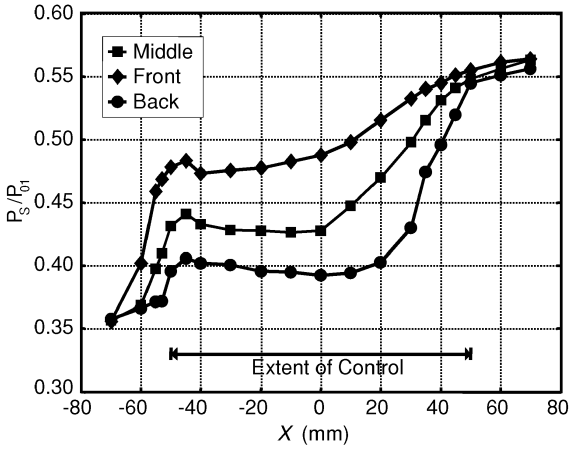

Fig. 17 Surface-pressure distributions (shock located at $x = -17$ and 17).

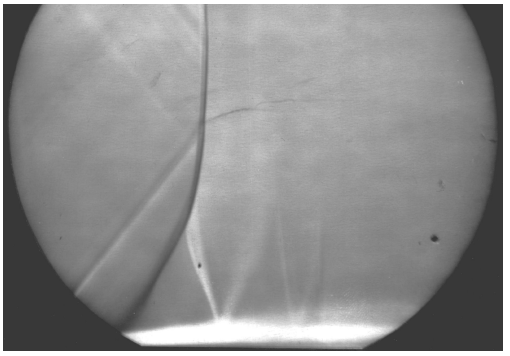

a)

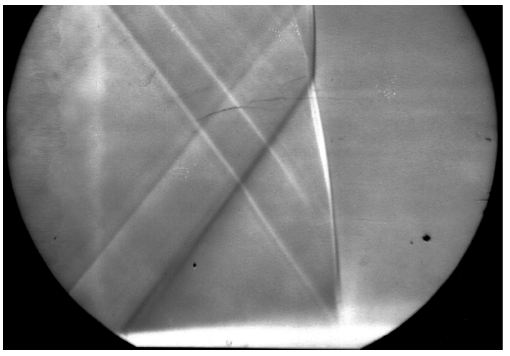

b)

Fig. 16 Schlieren pictures of controlled interaction; shock located at a) $x = -17$ and b) $x = 17$.

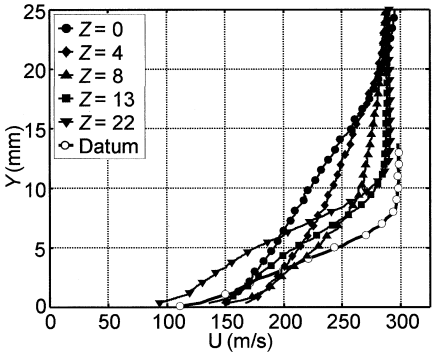

a)

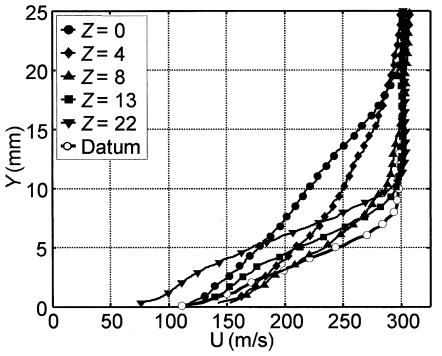

b)

Fig. 18 Boundary-layer velocity profiles ($x = 90$); shock located at a) $x = -17$ and b) $x = 17$.

Conclusions

It has been shown that the presence of streamwise slots located underneath a normal shock-wave/boundary-layer interaction causes a bifurcation of the shock structure. With increasing spanwise distance from the slot, the shock structure relaxes toward an uncontrolled interaction. However this relaxation is slow, and the influence of slots on the structure is global.

Boundary-layer velocity measurements indicate a local thickening of the boundary layer. This thickening is confined to a narrow region behind the slots, indicating that the effect of slots on the boundary layer is highly localized and suggests that only small viscous penalties are incurred compared to other flow-control devices incorporating wall transpiration, that is, passive control. Viscous losses can be decreased even further by increasing the slot spacing.

Outside the boundary layer a reduction in total pressure loss was observed at all spanwise locations as a result of the bifurcated shock structure, whereas the total pressure loss is only increased in a narrow region behind the slots.

The boundary-layer flow is highly three-dimensional and is dominated by a counter-rotating vortex pair. The presence of this vortex pair and its beneficial effect on the boundary layer are likely to delay separation in flows with adverse pressure gradients.

The location of the shock wave relative to the slot has little effect on the boundary-layer development. Therefore, it would appear that for different shock locations the effectiveness of the control device is dependent upon the modified shock structure and the corresponding total pressure loss.

When applied to an aerofoil, the beneficial effects of the control can outweigh the increased viscous drag and lead to a reduction in total drag. The spanwise spacing of slots on a wing should be sufficiently large to minimize the increase in viscous drag, while still producing a bifurcation of the shock structure between slots.

Acknowledgment

This work was performed with the financial assistance of the Engineering and Physical Sciences Research Council, United Kingdom.

References

[1]Rosemann, H., Knauer, A., and Stanewsky, E., "Experimental Investigation of the Transonic Airfoils DA LVA1-1A and VA-2 with Shock Control," *Notes on Numerical Fluid Mechanics*, Euroshock—Drag Reduction by Passive Shock Control, Vol. 56, edited by E. Stanewsky, J. Delery, J. Fulker, and W. Geissler, Vieweg, Brunswick, Germany, 1997, pp. 355–378.

[2]Fulker, J. L., and Simmons, M. J., "An Experimental Investigation of Passive Shock/Boundary Layer Control on an Aerofoil," *Notes on Numerical Fluid Mechanics*, Euroshock—Drag Reduction by Passive Shock Control, Vol. 56, edited by E. Stanewsky, J. Delery, J. Fulker, and W. Geissler, Vieweg, Brunswick, Germany, 1997, pp. 379–386.

[3]Raghunathan, S., "Passive Control of Shock-Boundary Layer Interaction," *Progress in Aerospace Sciences*, Vol. 25, No. 3, 1988, pp. 271–296.

[4]Delery, J. M., "Shock Phenomena in High Speed Aerodynamics: Still a Source of Major Concern," *The Aeronautical Journal*, Vol. 103, No. 1, 1999, pp. 19–34.

[5]Bohning, R., and Doerffer, P., "Hybrid and Active Control of the Shock Wave—Turbulent Boundary Layer Interaction and Porous Plate Transpiration Flow," Karlsruhe Univ. Euroshock II Final Technical Rept., Springer Verlag, New York, July 1999.

[6]Fulker, J. L., and Simmons, M. J., "An Investigation of Active, Suction, Shock and Boundary Layer Control Techniques," Euroshock II TR CT95-0095/3.1, Springer Verlag, New York, Jan. 1999.

[7]Delery, J. M., "Shock Wave/Turbulent Boundary Layer Interaction and its Control," *Progress in Aerospace Sciences*, Vol. 22, No. 4, 1985, pp. 209–280.

[8]Morris, M. J., Sajben, M., and Kroutil, J. C., "Experimental Investigation of Normal-Shock/Turbulent Boundary Layer Interactions with and Without Mass Removal," *AIAA Journal*, Vol. 30, No. 2, 1992, pp. 359–366.

[9]Thiede, P., and Dargel, G., "Assessment of Shock and Boundary Layer Control Concepts for Hybrid Laminar Flow Wing Design," Euroshock II TR BRPR-95-0076, Springer Verlag, New York, Sept. 1999.

[10]Ashill, P. R., and Fulker, J. L., "A Review of Flow Control Research at DERA," *Proceeding of IUTAM Symposium on Mechanics of Passive and Active Flow Control*, edited by G. E. A. Meier and P. R. Viswanath, Kluwer Academic, Norwell, MA, 1999, pp. 43–56.

[11]Qin, N., Zhu, Y., Ashill, P. R., and Shaw, S. T., "Active Control of Transonic Aerodynamics Using Suction, Blowing, Bumps and Synthetic Jets," AIAA Paper 2000-4329, Aug. 2000.

[12]Lee, B. H. K., "Self-Sustained Shock Oscillations on Airfoils at Transonic Speeds," *Progress in Aerospace Sciences*, Vol. 37, No. 2, 2001, pp. 147–196.

[13]Mabey, D. G., "Unsteady Aerodynamics: Retrospect and Prospect," *Aeronautical Journal*, Vol. 103, No. 1, 1999, pp. 1–18.

[14]de Nicola, C., "Introduction of Passive Shock Control in an Interactive Boundary Layer Method," *Notes on Numerical Fluid Mechanics*, Euroshock–Drag Reduction by Passive Shock Control, Vol. 56, edited by E. Stanewsky, J. Delery, J. Fulker, and W. Geissler, Vieweg, Brunswick, Germany, 1997, pp. 171–194.

[15]Ashill, P. R., Fulker, J. L., and Hackett, K. C., "Research at DERA on Sub Boundary Layer Vortex Generators (SBVGS)," AIAA Paper 2001-0887, Jan. 2001.

[16]Pearcey, H. H., "Shock Induced Separation and its Prevention," *Boundary Layer and Flow Control*, edited by G. V. Lachmann, Pergamon, 1961, pp. 1170–1355.

[17]Atkin, C. J., and Squire, L. C., "A Study of the Interaction of a Normal Shock Wave with a Turbulent Boundary Layer at Mach Numbers Between 1.3 and 1.55," *European Journal of Mechanics B/Fluids*, Vol. 11, No. 1, 1992, pp. 93–118.

[18]Sun, C., and Childs, M. E., "A Modified Wall Wake Velocity Profile for Turbulent Compressible Boundary Layers," *Journal of Aircraft*, Vol. 10, No. 6, 1970, pp. 381–383.

[19]Coles, D., "The Law of the Wake in the Turbulent Boundary Layer," *Journal of Fluid Mechanics*, Vol. 1, Pt. 2, 1956, pp. 191–226.

[20]Gibson, T. M., Babinsky, H., and Squire, L. C., "Passive Control of Shock Wave Boundary Layer Interactions," *The Aeronautical Journal*, Vol. 104, No. 3, 2000, pp. 129–140.

[21]Schubauer, G. B., and Spangenberg, W. G., "Forced Mixing in Boundary Layers," *Journal of Fluid Mechanics*, Vol. 8, Pt. 1, 1959, pp. 10–52.

[22]McCormick, D. C., "Shock/Boundary-Layer Interaction Control with Vortex Generators and Passive Cavity," *AIAA Journal*, Vol. 31, No. 1, 1993, pp. 91–96.

[23]Stanewsky, E., "Aerodynamic Benefits of Adaptive Wing Technology," *Aerospace Science and Technology*, Vol. 4, No. 7, 2000, pp. 439–452.